

Surface Pressures on a Flat Plate with Dual Jet Configurations

Joseph A. Schetz* and Antoni K. Jakubowski†
Virginia Polytechnic Institute and State University
Blacksburg, Virginia

and
Kiyoshi Aoyagi‡
NASA Ames Research Center, Moffet Field, California

A jet in a crossflow is of interest in numerous practical situations including jet powered VTOL aircraft. Two aspects of the problem have received little prior study, first, the effect of jet angle to crossflow, and second, the performance of dual-jet configurations both in line and side by side. The test plan for this work was designed to address these two aspects. The experiments were conducted in the Ames 7×10 ft Wind Tunnel at velocities ranging from 14.5 to 35.8 m/s (47.6 to 117.4 ft/s). Detailed pressure distributions are presented for single and dual jets having velocity ratios ranging from 3 to 8, spacings ranging from 2 to 6 diameters, and injection angles of 90, 75, and 105 deg. Shown here are the effects of the various parameters, as well as the contrasting effects of axisymmetric and flat plate geometries on the nature, size, shape, and strength of the interaction regions on the body surfaces.

Nomenclature

C_p	= pressure coefficient
ΔC_p	= pressure coefficient difference, ($C_{p_{jet on}} - C_{p_{jet off}}$)
D	= diameter
\dot{m}	= mass flow rate
P	= pressure
q	= dynamic pressure
R	= nominal velocity ratio
S	= center to center jet spacing
T	= temperature
V	= velocity
x	= streamwise coordinate measured from center of the front nozzle
X	= x/D
y	= transverse coordinate measured from nozzle center; plus (+) is to the right, looking downstream
y	= y/D
δ	= boundary layer displacement thickness
θ	= injection angle measured upwards from the horizontal, looking downstream
ρ	= density
<i>Subscripts</i>	
b	= main body
j	= jet conditions
∞	= freestream conditions
$()$	= average quantity over jet exit

Introduction

THE flowfield of a jet in a crossflow is of interest in a number of practical situations, including smokestacks, sewage outfalls, chemical mixing operations, and jet powered

VTOL aircraft. The available information on this general flow is discussed in Ref. 1. Since, for the VTOL application, the pressure field induced on adjacent surfaces is of particular importance, there have been a number of detailed experimental studies of that part of the flowfield covering many of the important variables and parameters.²⁻¹² Reviews of the early work can be found in Refs. 13 and 14, and a tabulation of the available information is contained in Ref. 15. The jet generally induces negative (with respect to the freestream) pressures on the nearby surfaces, and this results in a net loss of lift on the body viewed as a whole. The longitudinal variation of the surface pressures is also important, since that determines the resulting pitching moment.

There are two aspects of the general problem that have received little careful study. The first is the effect of jet angle with respect to crossflow. This effect is important because the transition to wingborne operation is usually accompanied by a change in the angle of the jet thrust vector. There are few prior investigations in the literature.^{8,11,16} The second item is the performance of dual jet configurations, either in line or side by side. The mutual interference as a function of center to center spacing is the issue here. Again, few references exist.^{3,8,17} Also, the interplay of these two items over a range of the key parameter for all such flows ($R = V_{jet}/V_{stream}$) is clearly of importance to the designer.

There have also been analyses, both conventional and semiempirical, of the jet in a crossflow problem.^{15,19,28} However, at the moment none can treat in a fundamental way a combination of the two items selected here for study. The experimental studies reported here should aid in the generalization of the existing analyses.

The test plan for the present work was designed to provide new information on the influence of the two effects chosen for investigation: 1) injection angle, and 2) in line and side by side jets.

Apparatus

Facility

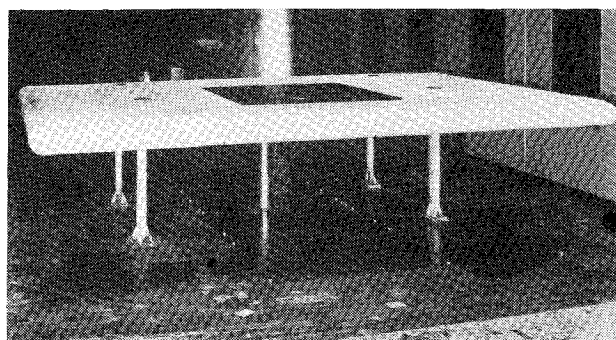
The experiments were conducted in the 7×10 ft (2.13×3.05 m) Subsonic Wind Tunnel at the NASA Ames Research Center at velocities ranging from 14.5 to 35.8 m/s (47.6 to 117.4 ft/s) depending upon the jet/freestream velocity ratio desired. This facility is described in Ref. 29.

Received July 29, 1983; revision received Dec. 29, 1983; Copyright © American Institute of Aeronautics and Astronautics, Inc., 1984. All rights reserved.

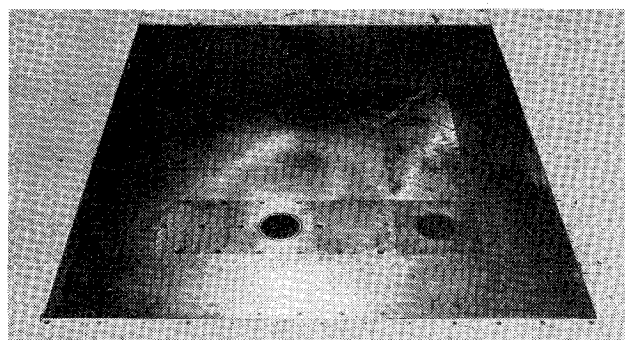
*Professor and Head, Aerospace and Ocean Engineering Department, Associate Fellow AIAA.

†Associate Professor, Aerospace and Ocean Engineering Department, Member AIAA.

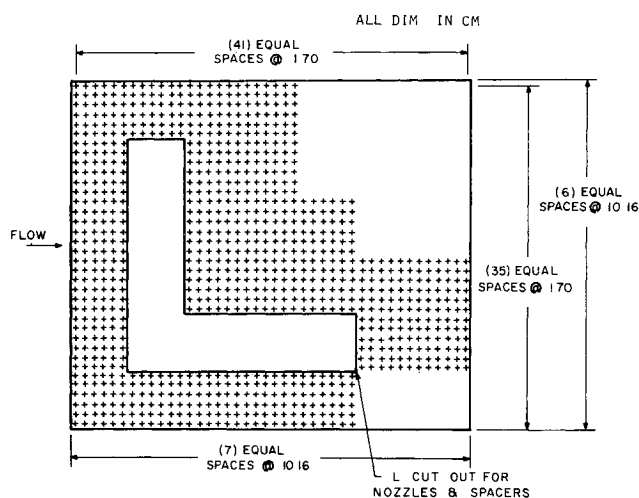
‡Aerospace Engineer, Member AIAA.



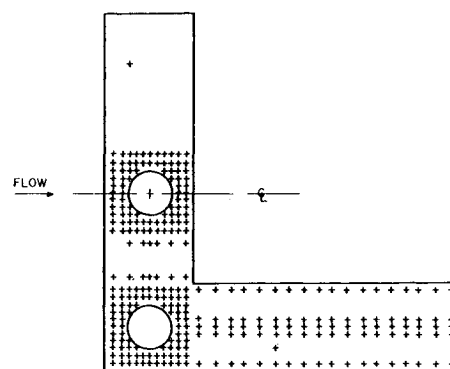
a) Photograph of the model in the wind tunnel



b) Close up of the nozzle section



c) Pressure top layout in the instrumented section of the model



d) Pressure top layout in the nozzle and space section

Fig 1 Flat plate model

Test Model

The model is shown in Fig 1. It has a streamlined leading edge and the bottom is covered with a fairing. There is a large L shaped cutout section created to accommodate the injector and spacer sections in various combinations. These combinations produce the required different center to center jet spacings in either the aligned or side by side arrangements. Each nozzle is located in a 10 16 cm (4 0 in) square section. There are a number of spacer sections either 5 08 cm (2 0 in) or 10 16 cm (4 0 in) long occupying the areas ahead of between, and behind the nozzle sections in the arrangements for the various jet spacings. The jets had a 4 92 cm (1 94 in) exit diameter. The front (or looking downstream the right) injector section always remained in the same place. The pressure tap layouts for the injector and spacer sections are shown using the 90 deg injector as an example. Part of the fixed portion of the plate is also instrumented with pressure taps.

A relatively uniform jet exit velocity profile for all injection angles was desired since nonuniformities in jet exit profiles have been shown to influence the surface pressure field.¹² The injector design finally chosen is shown for the 90 deg injector in Fig 2. The air is supplied via four tubes that entered the bottom. The air leaves the vents through four holes around the vent periphery. This configuration was selected in an attempt to distribute the entering flow over the cross section of the short (in the flow direction) plenum. Located above the vent exits is a perforated plate with the hole pattern shown which serves as the next step in the flow distribution process. This hole pattern was refined by trial and error and different patterns were required for the other injection angles. Above the perforated plate is a smooth contraction which runs down to the jet diameter. This is followed by a flow straightener

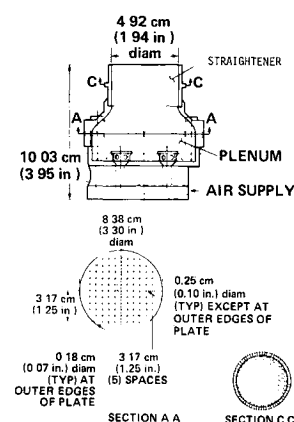


Fig 2 Details of the injection design for the 90 deg case

insert which consists of a thin wall tube holding a honeycomb with screening top and bottom. The purpose of the large length/diameter honeycomb is to force all of the flow in the same direction. The purpose of the screens is to lessen any remaining nonuniformities by accelerated turbulent mixing.

The primary instrumentation for all the tests was a group of 48 port Scanivalves. The integrity of each Scanivalve lead line from the pressure taps was carefully checked on a one by one basis by applying a known pressure to the tap at the model surface and reading the output from the Scanivalve. The Scanivalves were operated and the data was obtained iteratively by the data acquisition system for the 40 x 80 and 7 x 10 ft wind tunnels at Ames Research Center. All the data was recorded on tape for subsequent data reduction.

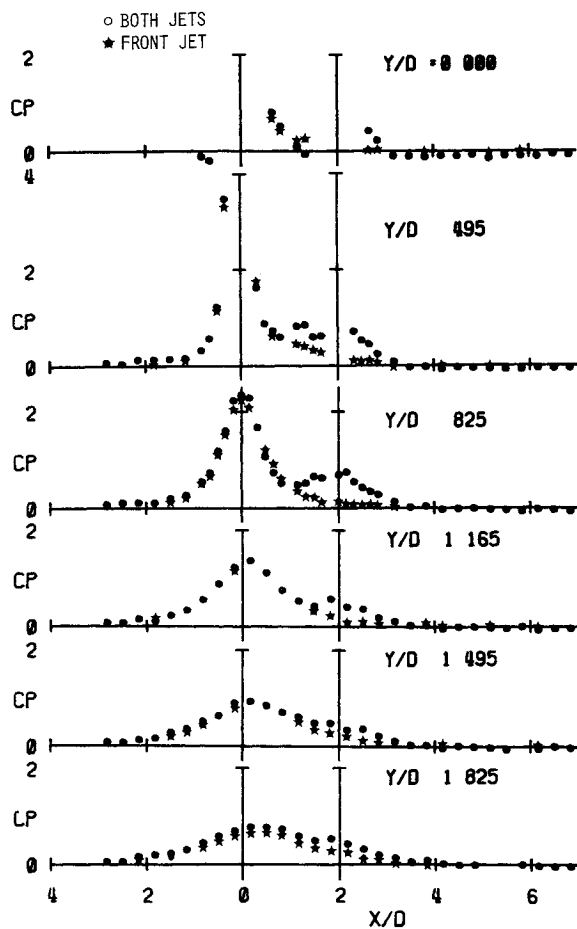


Fig 3 Surface pressure distribution (ΔC_p), flat plate model, 90 deg; $R=6$, $S/D=2$

All the other necessary measurements were also run through the data acquisition system. These included pressure measurements for tunnel speed, orifice readings for injector mass flow, and temperature readings for the tunnel and in injector air flows. The barometer and room temperature were read by eye and the information was entered manually into the data acquisition system.

Test Plan and Procedures

The desired range of jet to freestream velocity ratios can be obtained by a variety of paths, including holding the freestream velocity constant and varying the jet velocity or vice versa. Testing at a constant freestream velocity is attractive because that would keep the body Reynolds number and hence, the boundary layer thickness constant. However, the difficulties and effort required to achieve reasonably uniform jet exit velocity profiles over a 3:1 ($3 \leq R \leq 8$) range in jet average velocity was judged to be so severe as to justify the choice of holding the jet velocity fixed and varying the freestream. As a check on the influence of the body Reynolds number variation thus introduced, one case at the same R but with different freestream velocity, was included for most configurations tested. Only small effects were found.

There were three other constraints that influenced the test plan. First, it was considered important to keep the minimum body Reynolds number, based on the surface distance to the first nozzle above roughly 5×10^5 in order to have a turbulent boundary layer. This meant a freestream velocity above a value of about 13 m/s. Second, to avoid the added complexity of strong compressibility effects, it was decided to keep the maximum jet velocities roughly below 120 m/s ($M_j < 0.35$).

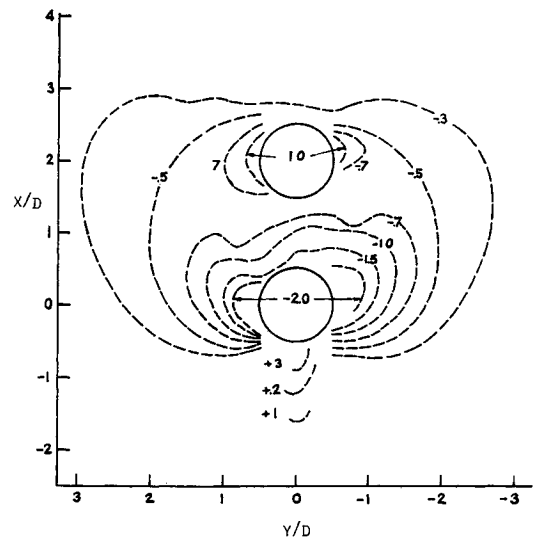


Fig 4 Isobar map of ΔC_p , flat plate with both jets 90 deg; $R=4$, $S/D=2$

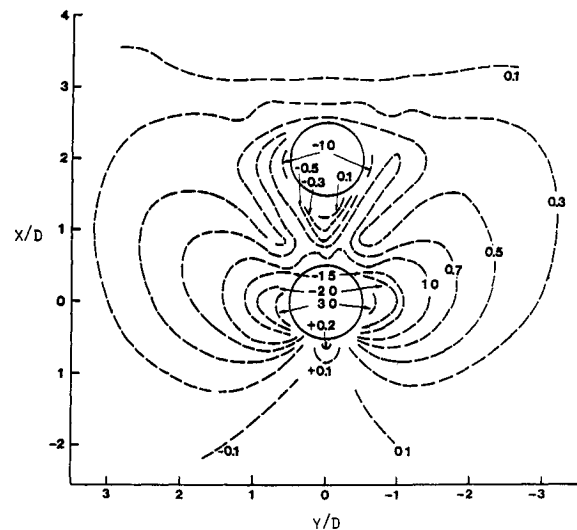


Fig 5 Isobar map of ΔC_p , flat plate with both jets 90 deg; $R=6$, $S/D=2$

Lastly, the pressure drop through the most severely inclined injectors was large enough to limit the mass flow (and thus the jet velocity) that could be obtained for those configurations.

Taking all of the items above into account, a test plan was adopted which had a nominal jet volume flow rate of 0.214 m³/s corresponding to $\bar{V}_j = 112.5$ m/s and freestream velocities corresponding to $1.28 \leq q \leq 8.03$ cm H₂O ($14.5 \leq V_\infty \leq 36.2$ m/s).

Each test series was run as follows. First, the data acquisition system was run to obtain 'null' readings and calibration settings. The air supply pressure settings corresponding to the set of injectors in use were then brought up and adjusted. Next, the tunnel was turned on to the lowest speed in the series. The data acquisition system was run. The tunnel speed was adjusted to the next setting and the process was repeated over the range desired. The last point in each series was a single value of R achieved at a combination of tunnel and jet speed different from the point at the same R in the main series. The tunnel and air supply were turned off and 'null' readings were again taken.

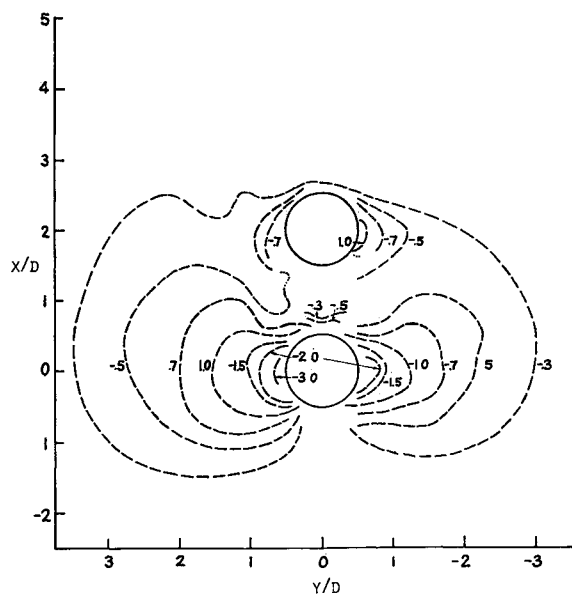


Fig 6 Isobar map of ΔC_p flat plate with both jets, 90 deg; $R=8$, $S/D=2$

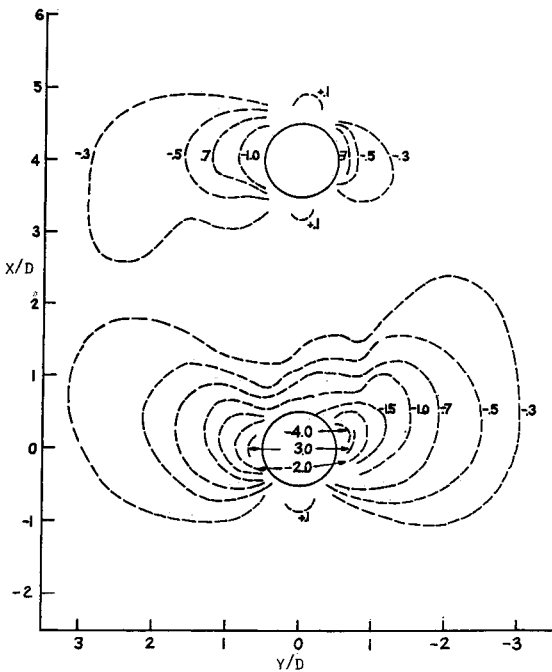


Fig 8 Isobar map of ΔC_p flat plate with both jets, 75 deg; $R=6$, $S/D=4$

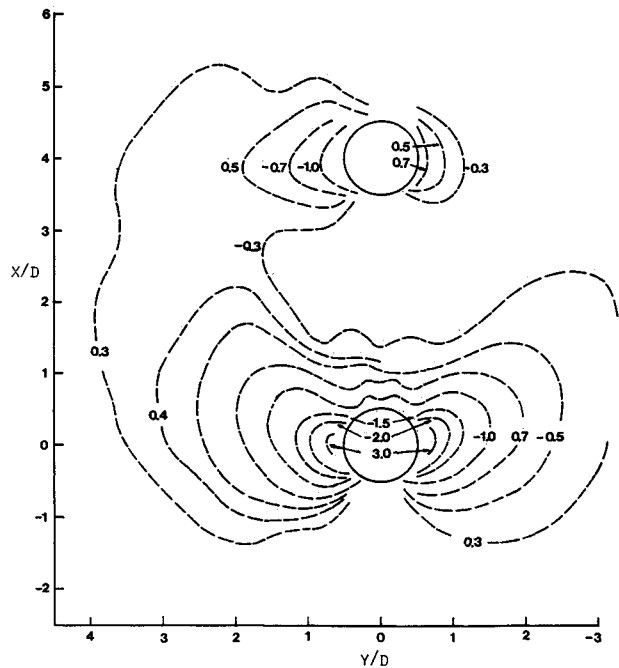


Fig 7 Isobar map of ΔC_p flat plate with both jets, 90 deg; $R=6$, $S/D=4$

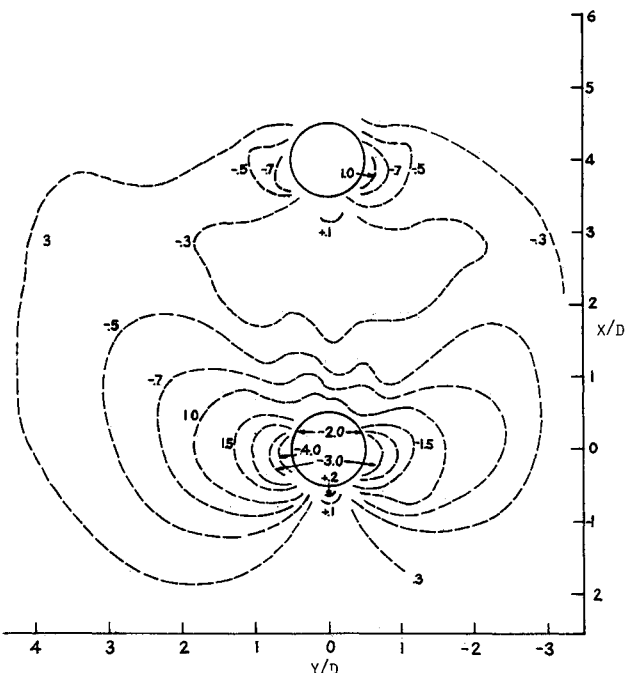


Fig 9 Isobar map of ΔC_p flat plate with both jets 105 deg; $R=6$, $S/D=4$

Results

The data were reduced and the results are presented here as

$$\Delta C_p = (C_{p_{jet\ on}} - C_{p_{jet\ off}})$$

which is a function of spatial location on the body surface for each configuration. In this way, the first order effects of any asymmetries or surface irregularities on the models should be normalized out. Before being accepted, each set of data was measured against certain criteria. For example, was the mass flow (and thus \tilde{V}_j) set close enough to the desired nominal conditions? For the two jet tests, were the mass flows set close enough to each other? (For these items, a tolerance of roughly $\pm 5\%$ was adopted.) When combined with the actual tunnel

speed for a given data point, was the desired value of R again achieved roughly $\pm 5\%$? These questions were important since we wished to make such case to case comparisons as the effect of jet spacing holding R nominally fixed, etc. Longitudinal pressure distributions at selected lateral distances are plotted in Fig 3 for the 90 deg injectors at $R=6$ with a spacing of two diameters and the jets aligned one behind the other. The results for both jets are shown as circles; those for the front jet are stars. Looking at the single jet results first, the expected pattern of negative ΔC_p 's is evident. The dual jet results show that the influence of the rear jet is less than that of the front jet at this

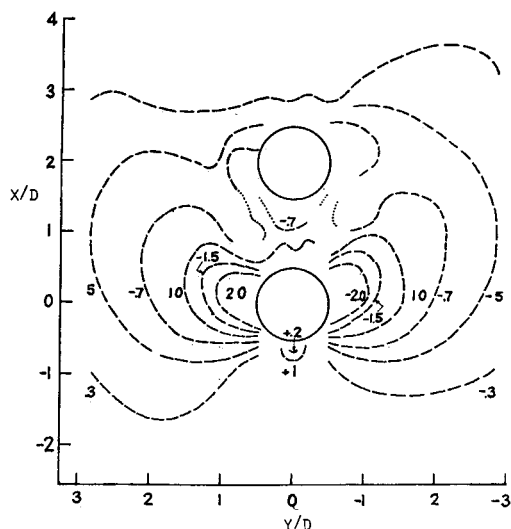


Fig 10 Isobar map of ΔC_p , flat plate with both jets, 75 deg; $R=6$, $S/D=2$

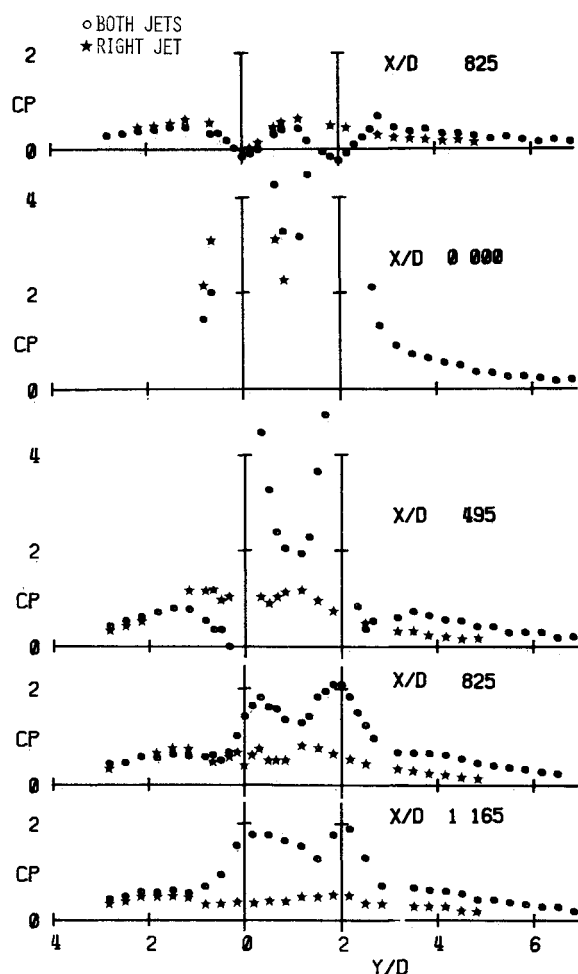


Fig 11 Transverse surface pressure distribution (ΔC_p) flat plate model, 90 deg; $R=6$, $S/D=2$ side by side

close spacing. On the other hand, the presence of the rear jet seems to strengthen the influence of the front jet slightly. The data in Fig 3 can be roughly compared to the data in Fig 6 of Ref. 30 for 90 deg injection with $S/D=2.0$ from a body of revolution at $R=7.7$. First, one finds that there are no positive ΔC_p values behind the second jet on the first plate. Second, the peak values on the body of revolution are

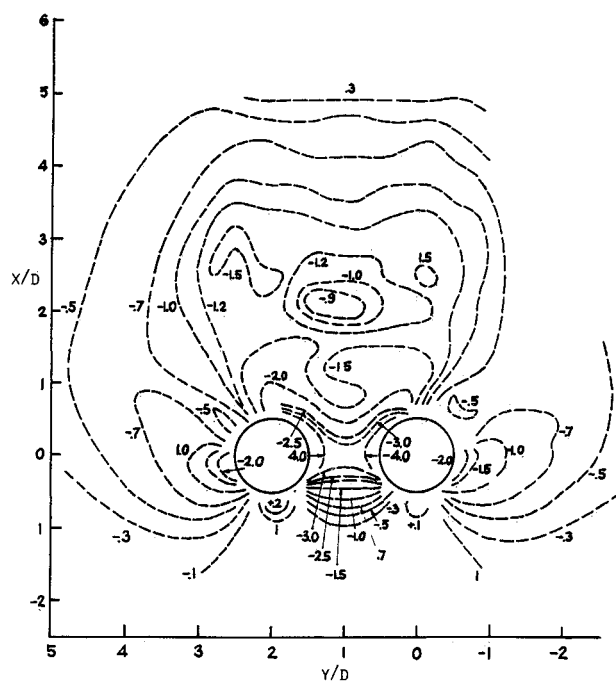


Fig 12 Isobar map of ΔC_p , flat plate with both jets, 90 deg; $R=6$, $S/D=2$, side by side

somewhat higher very near the nozzles. Third, by comparing values at $y/D=0.8$, it can be seen that the peak values decay faster with lateral distance on the body of revolution.

The effects of the important parameter R can be seen in the isobar plots in Figs 4, 5, and 6 for $R=4$, 6, and 8. As R increases, the area of the surface influenced by the jets increases. This increase is mostly in terms of the areas with small to moderate negative values of ΔC_p . The area with $\Delta C_p \leq -1.0$ does not change significantly with R . Since the area of influence increases with R , the total normal force also increases with R , but the increase is slow. Thus, the value of the total normal force normalized with the thrust of the jets actually decreases with increasing R . The effective center of normal force moves forward with increasing R . Estimates indicate that this center coincides with the center of the front jet at about $R=10$. Lastly, the shape of the interaction region changes with increasing R . At low R , the isobars show asymmetrical lobes displaced in the downstream direction. At higher R , there is less downstream distortion. Compare Fig 4 at $R=4$ to Fig 6 at $R=8$.

The present results in Fig 6 can be roughly compared with those of Wooler et al. in Ref. 31 at $R=8$, but with $S/D=2.5$ as opposed to our $S/D=2.0$. The comparison is made difficult since the tests in Ref. 31 did not have as detailed a coverage of the area near the jets. Nonetheless, comparison of the $\Delta C_p = -0.5$ isobars, for example, shows rather good agreement in terms of overall shape and axial and lateral extent.

The effects of increasing the dimensionless spacing S/D from 2 to 4 with 90 deg and $R=6$ are shown in Fig 7. Here, as for the body of revolution data in Ref. 30, the rear jet is still sheltered by the front jet, and the influence of the front jet on the flow is reduced by the presence of the rear jet. Looking at the isobar patterns in Fig 7 and comparing them with those in Fig 5 for the same case with $S/D=2$, it can be observed that the overlap of the interaction regions of the two jets is now for small ΔC_p values only. By comparing isobar plots with the front jet only (not presented here due to space limitations) with those for both jets operating, it is shown that the interaction of the two jets increases the surface area influenced by the front jet. It was also found that the merging of the interaction regions was influenced by the velocity ratio R . The merging is most pronounced at low R values. Also, the

sheltering of the rear jet reduces the downstream distortion of its flow interaction area

The influence of injection angle at $R=6$ is shown in the next two figures. Fig 8 has results for a 75 deg angle (15 deg downstream), and Fig 9 has results for injection at 105 deg (15 deg upstream), all at $S/D=4$. The isobar plots in Figs 8 and 9 and the plot for 90 deg in Fig 7 show some interesting effects. The change from 75 to 90 deg produces only slight changes in the total interaction area influenced by the jets and, thus, in the normal force. However, the change from 90 to 105 deg leads to an increase in the total interaction area and hence the normal force. Further as the angle goes from 75 to 90 to 105 deg, the effective center of the interaction region moves forward. The data indicate that the region ahead of the front jet is influenced somewhat more strongly by upstream angled injection. In addition the sheltering of the rear jet by the front jet is stronger for 105 deg than for the 90 or 75 deg injection.

The result of reduced spacing to $S/D=2$ at 75 deg and $R=6$ can be noted by comparing Fig 10 with Fig 8 for $S/D=4$. The effects are generally the same as for the 90 deg injection.

The next series of figures presents the results obtained with two jets in a side by side arrangement. Due to test time

limitations fewer parameters were varied in this configuration. All the data obtained are for the 90 deg injectors only.

Transverse pressure distributions at five axial stations including one ahead of the jets, are shown in Fig 11 for $R=6$ and $S/D=2$. Data for only the right jet operating are shown as solid circles. The presence of the left jet has a slight effect on the right jet at the station ahead of the jets ($x/D = -825$), but the interference effect is quite large at $x/D=0$ and the downstream stations. High (negative) ΔC_p values are obtained between and just downstream of the jets. Also the right/left symmetry of the flow was found to be good for single and dual jet runs. An isobar map for the same case is given in Fig 12.

Figures 13 and 14 show isobar maps for $S/D=2$ with $R=4$ and 8. By comparing these with the previous figure, the effects of R can be seen. As R is increased, there is a pronounced increase in the size of the interaction region around the jets. The interaction normal force also increases, both as a result of the increase in area affected and increases (negative) in the ΔC_p values near the orifices. The effective center of the interaction force shifts upstream as R is increased. Collectively, these results indicate a strong increase in

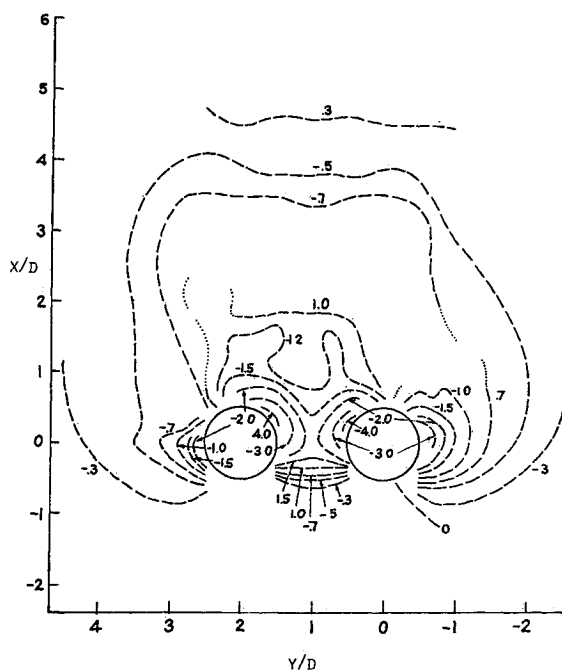


Fig 13 Isobar map of ΔC_p , flat plate with both jets, 90 deg; $R=4$, $S/D=2$, side by side

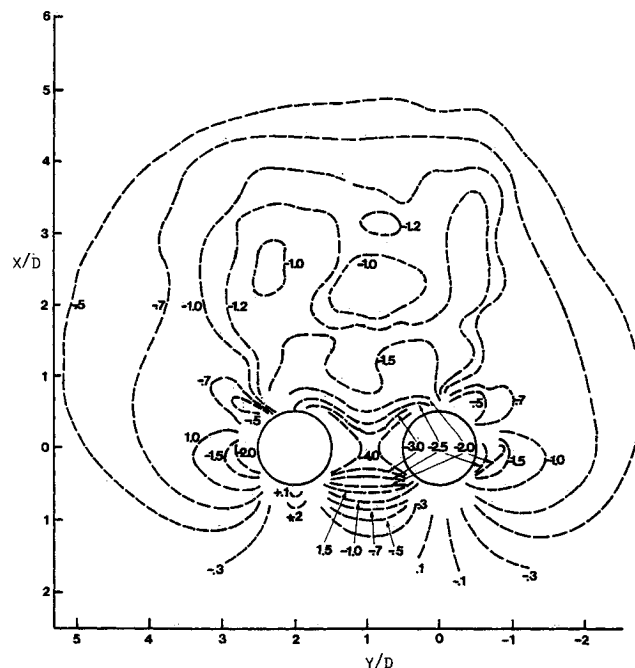
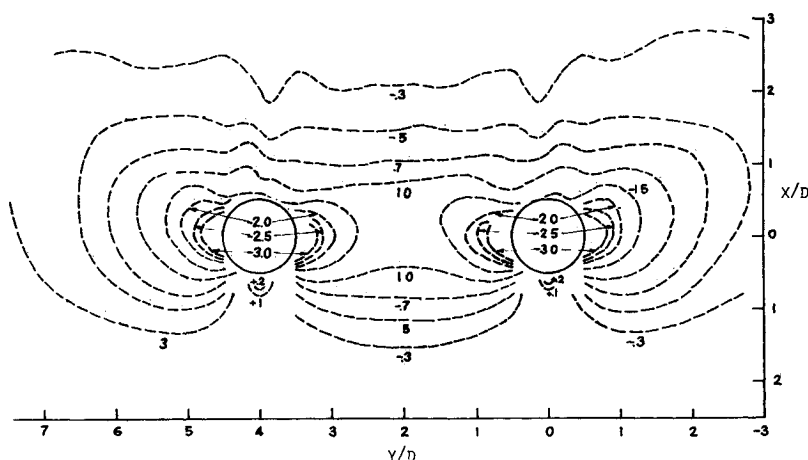


Fig 14 Isobar map of ΔC_p , flat plate with both jets, 90 deg; $R=8$, $S/D=2$, side by side

Fig 15 Isobar map of ΔC_p , flat plate with both jets, 90 deg; $R=6$, $S/D=4$, side by side



the interaction between the two jets as R is increased at this close spacing. The large (negative) ΔC_p values in the region immediately behind the jets along the line of symmetry between them at high R values are noteworthy. This is probably a result of the interaction between the pairs of counter rotating vortices formed in each jet.

The influence of increasing S/D to 4 at $R=6$ can be seen by comparing the results in Fig. 15 to those given earlier for $S/D=2$ at the same R in Fig. 12. The interaction of the jets is diminished significantly. Looking at the isobar maps, one can see that there is much less overlap of the interaction regions of the two jets at $S/D=4$. The overlap or merging of the interaction regions is R dependent; it is strongest at the higher R values. The interaction region of each jet on the "free" side (the side away from the other jet) is still always larger than for the single jet even at $S/D=4$. This is probably due to a blocking effect. The main flow approaching the side by side jets is partially "blocked" in the center region and "spilled over" around the sides resulting in more fluid flow and higher velocities (and lower pressures) on the free side of the jets.

Conclusions

In Line Jets

The mutual interaction of the jets results in sheltering of the rear jet by the front and in some cases "swelling" of the front jet because of the presence of the rear jet. Due to the latter effect, the surface area influenced by the front jet tends to be greater than for the case of a single jet.

Increasing R increases the surface area influenced by the jets and the effective center of the normal force moves forward with increasing R from a location between the jets to one near the center of the front jet at about $R=10$.

Obviously, increasing S/D diminishes the interaction effects of the jets.

Varying the injection angle from 75 to 90 to 105 deg moves the effective center of the interaction region forward. The upstream angled injection appears to strongly affect the overall pressure distributions.

Side By Side Jets

For the side by side jets, gross interaction features are characterized by two interrelated effects: 1) significantly enhanced flow velocity (and thus reduced surface pressures) between the jets due to the "channeling" of the flow between the jets, and 2) increased (when compared with the single jet) blocking of the crossflow and spill over to the sides which results in increased flow velocities (lower pressures) on the free sides of the jets.

Increasing R magnifies the interaction effects and the resulting forces. The downstream region, in particular, is strongly affected because of the strong interaction between the near wake portions of the jets.

Increasing S/D reduces the interaction effects.

References

- ¹Schetz, J. A. *Injection and Mixing in Turbulent Flow*. AIAA, New York, 1980.
- ²Vogler, R. D. 'Surface Pressures Distributions Induced on a Flat Plate by a Cold Air Jet Issuing Perpendicularly from the Plate and Normal to a Low Speed Free Stream Flow'. NASA TN D 1629, 1963.
- ³Vogler, R. D. 'Interference Effects of Single and Multiple Round or Slotted Jets on a VTOL Model in Transition'. NASA TN D 2380, 1964.
- ⁴Bradbury, L. J. S. and Wood, M. N. 'The Static Pressure Distributions Around A Circular Jet Exhausting Normally From a Plane Wall Into an Airstream'. C. P. No. 822, British A. R. C., 1965.
- ⁵Margason, R. J. 'Jet Induced Effects in Transition Flight'. Conference on V/STOL and STOL Aircraft. NASA SP 116, 1966, pp. 177-189.
- ⁶Gentry, Carl L. and Margason, Richard J. 'Jet Induced Lift Losses on VTOL Configurations Hovering In and Out of Ground Effect'. NASA TN D 3166, Feb. 1966.
- ⁷Soullier, A. 'Testing at SI MAS for Basic Investigation on Jet Interactions. Distributions of Pressure Around the Jet Orifice'. NASA TTF 14066, April 1968.
- ⁸Fricke, L. B., Wooller, P. T. and Ziegler, H. 'A Wind Tunnel Investigation of Jets Exhausting Into a Crossflow'. AFFDL TR 70 154, Vols. I-IV, U. S. Air Force, Dec. 1970.
- ⁹Margason, R. J. 'Review of Propulsion Induced Effects on Aerodynamics of Jet/STOL Aircraft'. NASA TN D 5617, Feb. 1970.
- ¹⁰Fearn, R. L. and Weston, R. P. 'Induced Pressure Distribution of a Jet in a Crossflow'. NASA TN D 7916, June 1975.
- ¹¹Taylor, P. 'An Investigation of an Inclined Jet in a Crosswind'. *Aeronautical Quarterly*, Vol. XXVIII, Part I, Feb. 1977.
- ¹²Kuhlman, J. M., Ousterhout, D. S. and Warcup, R. W. 'Experimental Investigation of Effects of Jet Decay Rate on Jet Induced Pressures on a Flat Plate: Tabulated Data'. NASA CR 158990, Nov. 1978.
- ¹³Lee, C. C. 'A Review of Research on the Interaction of a Jet With an External Stream'. [Contract No. DA 01 021 AMC 11528(z)] Research Lab., Brown Engineering Co., Inc. Tech. Note R 184, March 1966. (Available from DDC as AD 630 294).
- ¹⁴Garner, J. E. 'A Review of Jet Efflux Studies Application to V/STOL Aircraft'. U. S. Air Force AEDC-TR 67 163, Sept. 1967. (Available from DDC as AD 658 432).
- ¹⁵Perkins, S. C. Jr. and Mendenhall, M. R. 'A Study of Real Jet Effects on the Surface Pressure Distribution Induced by a Jet in a Crossflow'. NASA CR 166150, March 1981.
- ¹⁶Margason, R. J. 'The Path of a Jet Directed at Large Angles to a Subsonic Free Stream'. NASA TN D 4919, Nov. 1968.
- ¹⁷Ziegler, H. and Wooller, P. T. 'Analysis of Stratified and Closely Spaced Jets Exhausting into a Crossflow'. NASA CR 132297, Nov. 1973.
- ¹⁸Ousterhout, D. S. 'An Experimental Investigation of a Cold Jet Emitting from a Body of Revolution into a Subsonic Free Stream'. NASA CR 2089, July 1972.
- ¹⁹Abramovich, G. N. *The Theory of Turbulent Jets*. MIT Press, Co., 1963, pp. 541-552.
- ²⁰Wu, J. C. and Wright, M. A. 'A Blockage Sink Representation of Jet Interference Effects for Noncircular Jet Orifices. Analysis of a Jet in a Subsonic Crosswind'. NASA SP 218, 1969, pp. 85-99.
- ²¹Street, T. A. and Spring, J. 'Experimental Reaction Jet Effects at Subsonic Speeds. Analysis of a Jet in a Subsonic Crosswind'. NASA SP 218, 1969, pp. 63-83.
- ²²Dietz, W. E. Jr. 'A Method for Calculating the Induced Pressure Distribution Associated with a Jet in a Crossflow'. M. S. Thesis, Florida University, 1975. (also available as NASA CR 146434, 1975).
- ²³Yen, K. T. 'The Aerodynamics of a Jet in a Crossflow'. NADC 78291, 60 Dec. 1978.
- ²⁴Perkins, S. C. Jr. and Mendenhall, M. R. 'A Correlation Method to Predict the Surface Pressure Distribution on an Infinite Plate or a Body of Revolution from which a Jet is Issuing'. NASA CR 152345, Jan. 1980.
- ²⁵Fearn, R. L., Kalota, C. and Dietz, W. E. Jr. 'A Jet Aerodynamic Surface Interference Model'. *Proceedings V/STOL Aircraft Aerodynamics*, Vol. 1, Naval Post Graduate School, Monterey, Calif., May 1979.
- ²⁶Campbell, J. F. and Schetz, J. A. 'Analysis of the Injection of a Heated Turbulent Jet into a Cross Flow'. NASA TR R 413, Dec. 1973.
- ²⁷Baker, A. J., Manhardt, P. D. and Orzechowski, J. A. 'A Three-Dimensional Finite Element Algorithm for Prediction of V/STOL Jet Induced Flowfields'. AGARD Symposium, Lisbon, Portugal, Nov. 1981.
- ²⁸Isaac, K. M. and Schetz, J. A. 'Analysis of Multiple Jets in a Crossflow'. *Journal of Fluids Engineering*, Vol. 104, 1982, pp. 489-492.
- ²⁹7x10 Wind Tunnel Guide. Ames Research Center, NASA, Oct. 1978.
- ³⁰Schetz, J. A., Jakubowski, A. K., and Aoyagi, K. 'Jet Trajectories and Surface Pressures Induced on a Body of Revolution with Various Dual Jet Configurations'. *Journal of Aircraft*, Vol. 20, Nov. 1983, pp. 975-982.
- ³¹Wooller, P. T., Wasson, H. R., Kao, H. C., Ziegler, H., and Schwandemann, M. F. 'V/STOL Aircraft Aerodynamic Prediction Methods Investigation'. AFFDL-TR 72 26, Jan. 1972.